Supplemental Data

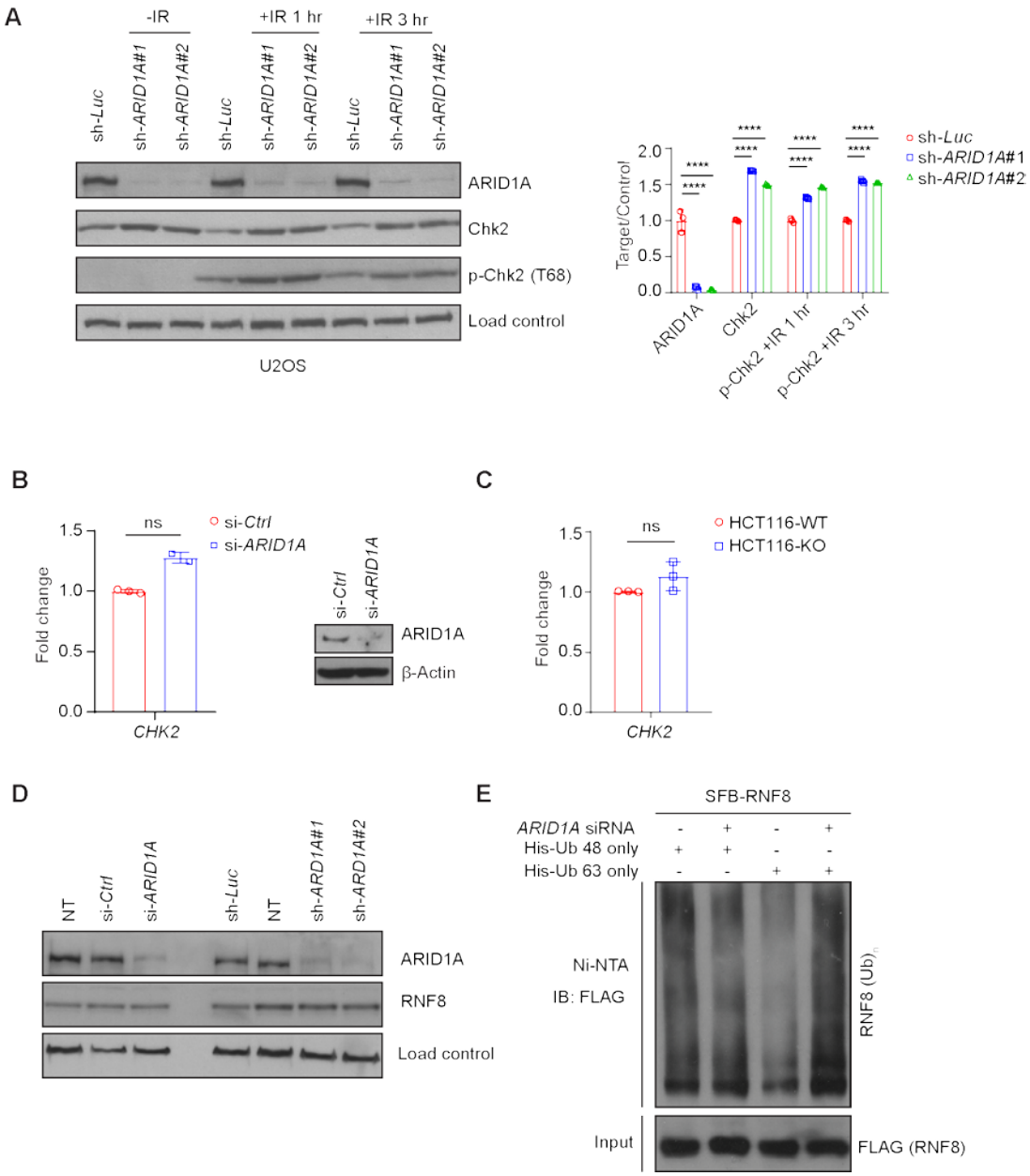

Supplemental Figure 1. Depletion of *ARID1A* does not affect *CHK2* mRNA level or RNF8 protein level. (**A**) Left, western blots of ARID1A, Chk2, and p-Chk2 in U2OS cells after exposure to 10 Gy ionizing radiation (IR). Right, quantitative analysis from normalization to loading control represent the mean ± SD (ARID1A, P<0.0001; Chk2, p<0.0001; p-Chk2, p<0.0001 by one-way ANOVA with Dunnett's multiple comparisons test). (**B**) Left, qPCR analysis of *CHK2* mRNA expression in U2OS cells. Right, western blots indicate effective ARID1A knockdown. si-Ctrl, si-Nontarget; Quantitative analysis represents the mean ± SD of three independent experiments. (**C**) *CHK2* mRNA expression in HCT116-WT and *ARID1A*-KO cells from RNA SEQ analysis. Quantitative analysis represents the mean ± SD of three independent experiments. Two-tailed unpaired Student's *t* test (**B** and **C**). (**D**) Western blots of ARID1A and RNF8 in transient and stable *ARID1A*-knockdown U2OS cells. NT, Nontreated; si-Ctrl, si-Nontarget. (**E**) Immunoblot of U2OS cells transfected with indicated plasmid and siRNA, SFB-tagged (S-tag, Flag epitope tag, and streptavidin-binding peptide tag) RNF8 (SFB-RNF8), si-Nontarget, or siRNA targeting *ARID1A* along with His-ubiquitin (His-Ub) 48 or His-Ub 63 constructs.

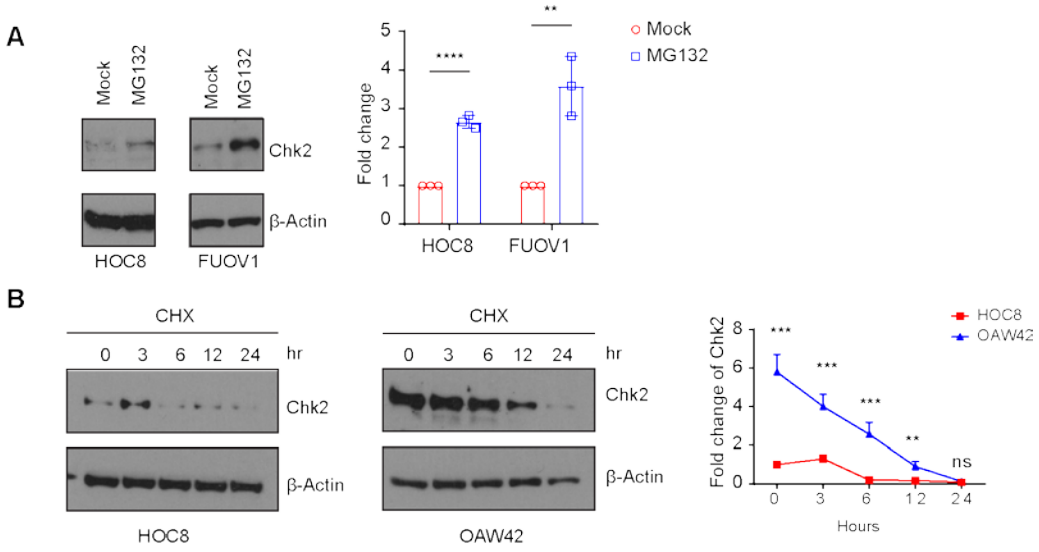

Supplemental Figure 2. Chk1 expression is not affected by *ARID1A* deficiency. (**A**) Left, western blots of Chk2 in ovarian cancer cell lines HOC8 and FUOV1 treated with MG132 (1 μM) for 6 hours. Right, quantitative results represent the mean ± SD of three independent experiments. **, P < 0.01; ****, P < 0.0001. (**B**) Western blots of Chk2 in ovarian cancer cell lines HOC8 (left) and OAW42 (middle) treated with cycloheximide (CHX) (25 μg/ml). Right, quantitative results represent the mean ± SD of three independent experiments. **, P < 0.01; ***, P < 0.001. Two-tailed unpaired Student's *t* test (**A** and **B**).

A

Chk2 protein sequence, red indicate the mutant K.

MSRESDVEAQQSHGSSACSQPHGSVTQSQGSSSQSQGISSSSTSTMPNSSQSSHSSSGTLSSLETVSTQE
LYSIPEDQEPEDQEPEEPTPAPWARLWALQDGFANLECVNDNYWFGRDKSCEYCFDEPLLKRTDKYRTYSK
KHFRIFREVGPKNSYIAYIEDHSGNGTFVNTELVGKGKRRPLNNNSEIALSLSRNKVFVFFDLTVDDQSVYPKA
LRDEYIMSKTLGSGACGEVKLAFERKTCKKVAIKIISKRKFAIGSAREADPALNVETEIEILKKLNHPCIIKIKNFFD
AEDYYIVLELMEGGELFDKVVGNKRLKEATCKLYFYQMLLAVQYLHENGIIHRDLKPENVLLSSQEEDCLIKITD
FGHSKILGETSLMRTLCGTPTYLAPEVLVSVGTAGYNRAVDCWSLGVILFICLSGYPPFSEHRTQVSLKDQITS
GKYNFIPEVWAEVSEKALDLVKKLLVVDPKARFTTEEALRHPWLQDEDMKRKFQDLLSEENESTALPQVLAQ
PSTSRKRPREGEAEGAETTKRPAVCAAVL

B

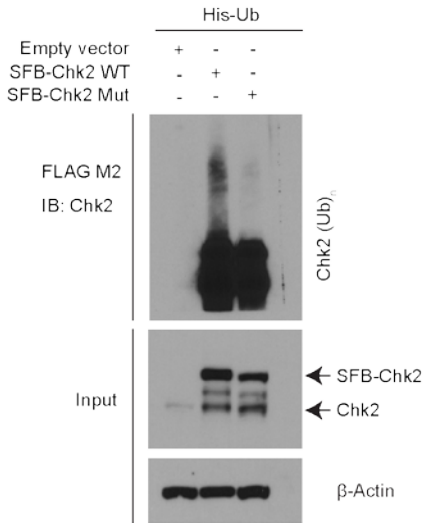

Supplemental Figure 3. Identification of Chk2 poly-ubiquitination sites. (**A**) Predictive Chk2 poly-ubiquitination sites. (**B**) Immunoblot of 293T cells transfected with indicated plasmid and siRNA, SFB-tagged (S-tag, Flag epitope tag, and streptavidin-binding peptide tag) Chk2 WT, SFB-Chk2 Mut (K492R, K494R, K520R and K534R) along with His-ubiquitin (His-Ub) constructs. IB, Chk2.

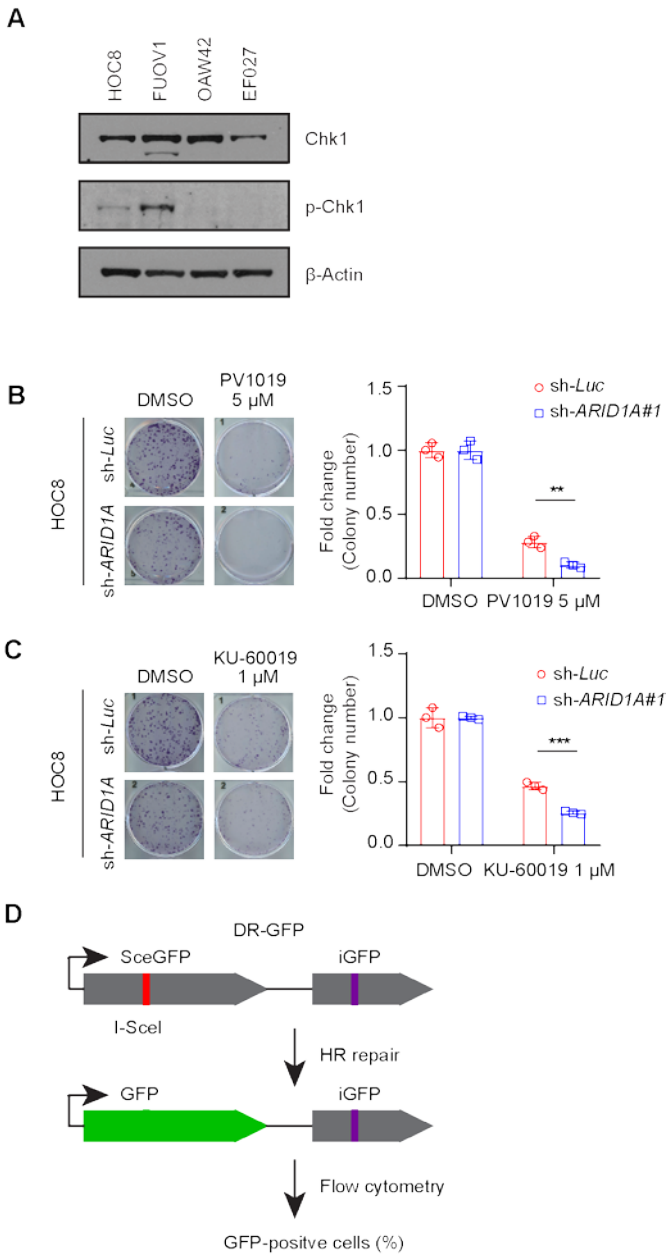

Supplemental Figure 4. Inactivation of ATM-CHK2 axis sensitizes ovarian cancer cells with *ARID1A* depletion. (**A**)Western blots of Chk1 in ovarian cancer cell lines with different levels of ARID1A. (**B-C**) *ARID1A*-knockdown HOC8 cells were treated with DMSO, PV1019 (**B**), or KU-60019 (**C**) at indicated concentrations. Clonogenic assays were performed. Left, representative images of colony formation. Right, quantitative results represent the mean ± SD from three independent experiments. **, P < 0.01; ***, p<0.001 by two-tailed unpaired Student's *t* test. (**D**) Schematic diagram of the DR-GFP reporter assays.

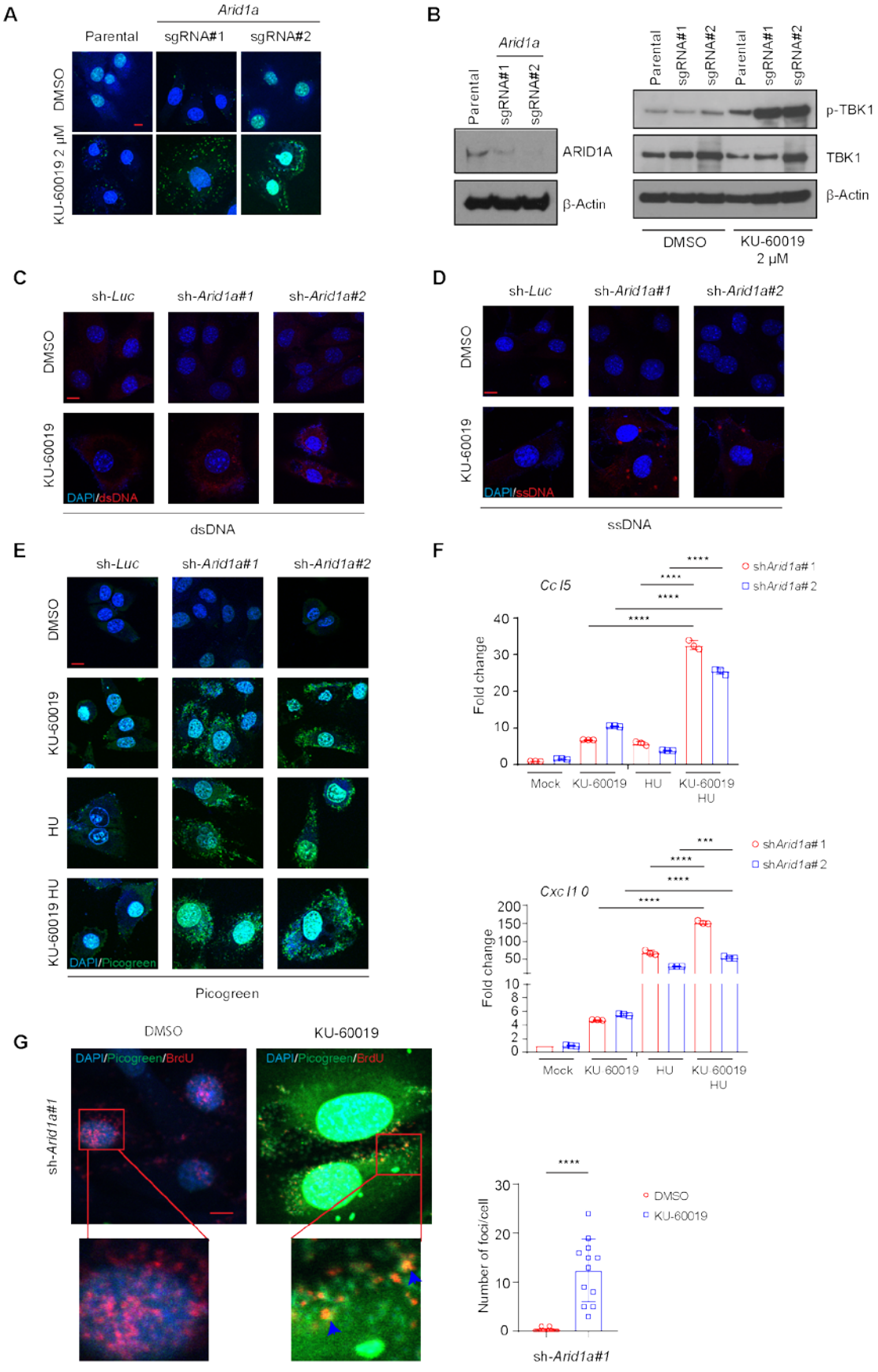
A
Arid1a
Parental
sgRNA#1
sgRNA#2
DMSO
KU-60019 2 μM
B
Arid1a
Parental
sgRNA#1
sgRNA#2
ARID1A
β-Actin
p-TBK1
TBK1
β-Actin
DMSO
KU-60019 2 μM
C
sh-Luc
sh-Arid1a#1
sh-Arid1a#2
DMSO
KU-60019
DAPI/dsDNA
dsDNA
D
sh-Luc
sh-Arid1a#1
sh-Arid1a#2
DMSO
KU-60019
DAPI/ssDNA
ssDNA
E
sh-Luc
sh-Arid1a#1
sh-Arid1a#2
DMSO
KU-60019
HU
KU-60019 HU
DAPI/Picogreen
Picogreen
F
Ccl5
shArid1a#1
shArid1a#2
Fold change
Mock
KU-60019
HU
KU-60019 HU
Cxcl10
shArid1a#1
shArid1a#2
Fold change
Mock
KU-60019
HU
KU-60019 HU
G
DMSO
KU-60019
sh-Arid1a#1
DAPI/Picogreen/BrdU
DAPI/Picogreen/BrdU
Number of foci/cell
DMSO
KU-60019
sh-Arid1a#1

Supplemental Figure 5. ATM inhibitor stimulates cytosolic DNA in ID8 *ARID1A*-KO cells. (**A**) Representative images of PicoGreen staining in parental and *Arid1a*-depleted (sgRNA#1 and #2) ID8 cells treated with DMSO or KU-60019 (2 μM) for 48. DAPI (blue) was used to visualize the nuclei. Scale bar, 10 μm. (**B**) Left, western blots indicate effective *Arid1a* knockdown. Right, western blots of phosphorylated TBK1 (p-TBK1) and total TBK1 (TBK1) in parental and *Arid1a*-depleted (sgRNA#1 and #2) ID8 cells treated with KU-60019 (2 μM) for 48 hours. (**C**-**D**) Representative images of dsDNA (**C**) and ssDNA (**D**) immunostaining in control (sh-*Luc*) and *Arid1a*-depleted (sh-*Arid1a*#1 and #2) ID8 cells treated with DMSO, KU-60019 (2 μM) for 48 hours. DAPI (blue) was used to visualize the nuclei. Scale bar, 10 μm. (**E**). Representative images of PicoGreen staining in control (sh-*Luc*) and *Arid1a*-depleted (sh-*Arid1a*#1 and #2) ID8 cells treated with DMSO, HU (2 mM), KU-60019 (2 μM) or combination treatment for 48 hours. DAPI (blue) was used to visualize the nuclei. Scale bar, 10 μm. (**F**) qPCR analysis of *Ccl5* and *Cxcl10* mRNA expression in *Arid1a* knockdown ID8 cells under DMSO, HU (2mM), KU-60019 (2 μM) or combination treatment for 48 hours. Data represent mean ± SD of three independent experiments. ***, $p<0.001$; ****, $p<0.0001$. (**G**) Left, Representative images of co-staining of BrdU and PicoGreen in *Arid1a* knockdown ID8 cells under DMSO or KU-60019 treatment. Right, quantitative results represent the mean ± SD of three independent experiments. ****, $p<0.0001$. ($n = 12$). Scale bar, 10 μm. One-way ANOVA with Sidak's multiple comparisons test (**E** and **F**), two-tailed unpaired Student's *t* test (**G**).

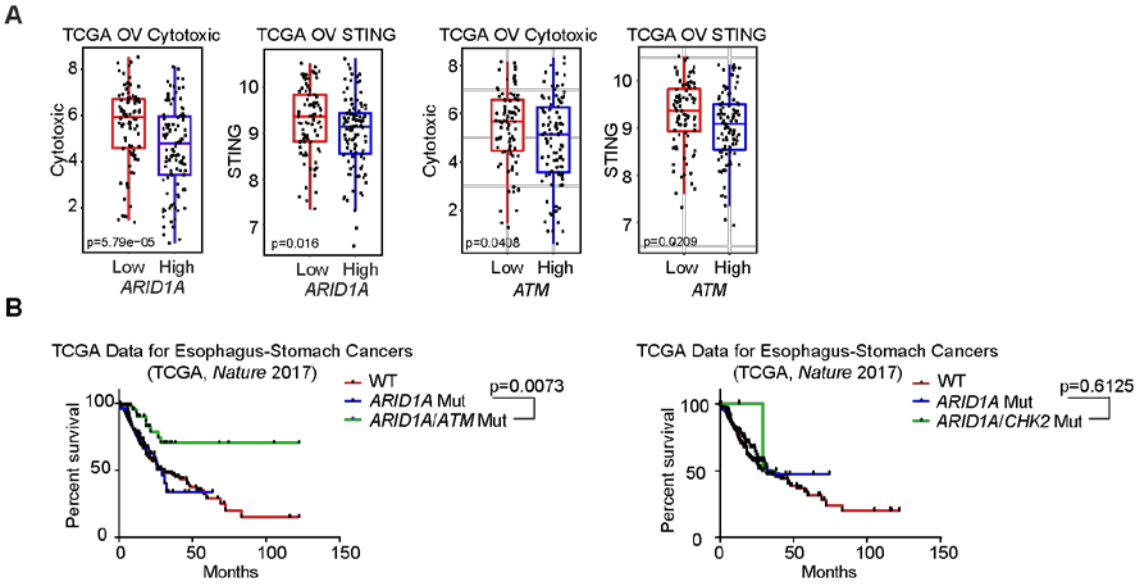

Supplemental Figure 6. Inhibition of the ATM-Chk2 axis promotes TIL signatures. (**A**) Associations between different subsets of TIL signatures and *ARID1A* or *ATM* mRNA expression in TCGA ovarian (OV) tumors (*n* = 309). The figures show associations of increased Cytotoxic and STING mRNA with reduced *ARID1A* or *ATM* mRNA expression (*ARID1A*: Cytotoxic p=5.79e^{-05}, STING p=0.016; *ATM*, Cytotoxic p=0.0408, STING p=0.0209). (**B**) Survival analysis for patients with esophagus or stomach cancer with *ARID1A*, *ATM*, and *CHK2* mutation (Mut). (Esophagus-Stomach, *n* = 518, *ARID1A*/*ATM* Mut (*n* = 19) vs *ARID1A* Mut (*n* = 63), p=0.0073; *ARID1A*/*CHK2* Mut (n=5) vs *ARID1A* Mut (*n* = 101), p=0.6125). Two-tailed unpaired Student's *t* test (**A** and **B**).

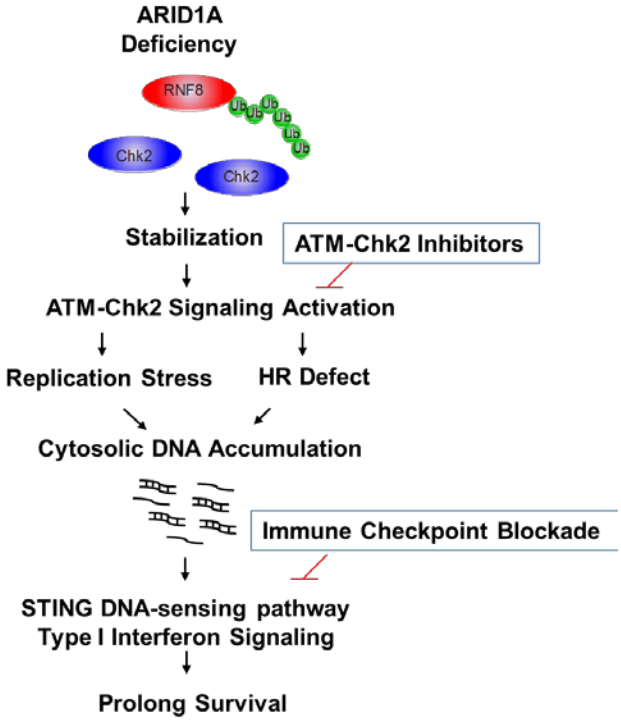

Supplemental Figure 7. Proposed model by which inhibition of ATM-Chk2 potentiates the efficacy of ICB therapy in *ARID1A*-deficient cancers.